HHS Public Access

Author manuscript

Ultrasound Med Biol. Author manuscript; available in PMC 2023 June 01.

Published in final edited form as:

Ultrasound Med Biol. 2022 June ; 48(6): 1058–1069. doi:10.1016/j.ultrasmedbio.2022.02.002.

Contrast enhanced ultrasound reveals partial perfusion recovery after hindlimb ischemia as opposed to full recovery by laser Doppler perfusion imaging

Alyssa B. Becker[1], **Lanlin Chen**[1], **Bo Ning**[1], **Song Hu**[1], **John A. Hossack**[1], **Alexander L. Klibanov**[1,2], **Brian H. Annex**[1,2], **Brent A. French**[1,2,*]

[1] Department of Biomedical Engineering, University of Virginia, Charlottesville, Virginia, United States of America

[2] Department of Medicine, Cardiovascular Division, University of Virginia, Charlottesville, Virginia, United States of America

Abstract

Mouse models are critical in developing new therapeutic approaches to treat peripheral arterial disease (PAD). Despite decades of research and numerous clinical trials, the efficacy of available therapies is limited. This may suggest shortcomings in our current animal models and/or methods of assessment. We evaluated perfusion measurement methods in a mouse model of PAD by comparing laser Doppler perfusion imaging (LDPI, most common technique), contrast enhanced ultrasound (CEUS, emerging technique), and fluorescent microspheres (conventional standard). Mice undergoing a femoral artery ligation were assessed by LDPI and CEUS at baseline, 1, 4, 7, 14, 28, 60, 90, and 150 days post-surgery to evaluate perfusion recovery in the ischemic hindlimb. 14 days post-surgery, additional mice were measured by fluorescent microspheres, LDPI, and CEUS. LDPI and CEUS showed broadly similar trends of perfusion recovery until 7 days post-surgery. However, by day 14, LDPI indicated a full recovery of perfusion, whereas CEUS showed a ~50% recovery which failed to improve even after 5 months. In agreement with the CEUS results, fluorescent microspheres at day 14 post-surgery confirmed that perfusion recovery was incomplete. Histopathology and photoacoustic microscopy provided further evidence of sustained vascular abnormalities.

Keywords

Perfusion imaging; ultrasound; ischemia; peripheral arterial disease

[*]Corresponding author: Brent A. French, PhD, MR5 Building, Room 1219, P.O. Box 800759, Charlottesville, Virginia 22908, bf4g@virginia.edu, Phone: +1 434-924-5728.

Introduction

Peripheral arterial disease (PAD) is caused by obstructions to blood flow due to atherosclerosis (Ouriel 2001). It primarily occurs in the legs, but can also occur in the upper extremities. PAD affects over 200 million people worldwide and has very limited treatment options (Fowkes et al. 2013). Many therapeutic approaches fail in clinical trials, suggesting that preclinical models and assessment methods may be imperfect (Iyer and Annex 2017; Krishna et al. 2016).

Mouse models of PAD are widely used and typically consist of a unilateral ligation(s) of the femoral artery to induce hindlimb ischemia (HLI) (Krishna et al. 2016). There are a variety of perfusion measurement techniques that can be applied to HLI models. Fluorescent (or radioactive) microspheres are the conventional standard for regional perfusion measurements. Microspheres are injected into arterial circulation and lodge in the capillaries in proportion to perfusion. They can be quantified ratiometrically or absolutely, under certain conditions (Cardinal and Hoying 2007). Microspheres are commonly used in large animal studies, however very few groups use them in mice because of the low flow velocities and small blood volumes in mouse skeletal muscle (Prinzen 2000). The microsphere technique also necessitates euthanasia for tissue acquisition, making serial studies more cumbersome and thus leading to the use of alternative methods by most groups using HLI models.

Laser Doppler perfusion imaging (LDPI) is the most commonly used technique to evaluate perfusion recovery after HLI in mice. LDPI is a simple to use optical technique. The output is a heat map of perfusion in the area of interest, which is typically the feet in most studies of HLI conducted in mice (Briers 2001). A limitation of LDPI is that measurements are typically made in the feet, whereas biochemical, histochemical and functional studies of HLI typically interrogate the muscles in the leg. Since LDPI is an optical technique, an inherent constraint is the limited depth of tissue that can be interrogated (~700 μm) (Davis et al. 2014; Senarathna et al. 2013). It should be noted that there are a number of newer optical techniques, such as spatial frequency domain imaging (Leyba et al. 2021) and Doppler optical coherence tomography (Rollins et al. 2002), that have greater tissue penetration depth. However, LDPI remains the most widely used technique to date.

A promising alternative technique for perfusion measurements in HLI models is contrast enhanced ultrasound (CEUS). CEUS is a well-established technique for assessing perfusion and has been applied clinically for coronary artery disease (Schinkel et al. 2016), peripheral arterial disease (Krix et al. 2005; Kundi et al. 2017), and cancer applications (Halpern 2006), as well as preclinically for kidney (Sullivan et al. 2009), adipose (Baron et al. 2012), heart (French et al. 2006), and tumor perfusion measurements (Pysz et al. 2011). The contrast agent is a microbubble with a lipid shell and gas core that remains purely intravascular. Microbubbles are best visualized in a nonlinear (harmonic) contrast mode that is available on many clinical scanners. CEUS is well suited for perfusion measurements in skeletal muscle, but it has yet to be widely adopted (Baltgalvis et al. 2014; Karvinen et al. 2011; Kuliszewski et al. 2011; Rissanen et al. 2008). A few groups have pioneered CEUS techniques for perfusion measurements (Cao et al. 2015; Kuliszewski et al. 2011; Leong-Poi

et al. 2005; Ryu et al. 2013; Smith et al. 2012), but it has yet to be commonly implemented in the assessment of HLI models (Aref et al. 2019). CEUS has the potential to overcome several of the limitations of LDPI, as well as add the resolution needed to evaluate perfusion on a per muscle basis.

Here, we test the hypothesis that CEUS can be used to serially assess perfusion recovery in a mouse HLI model of PAD. We measured perfusion recovery over time by LDPI and CEUS, then compared the results to traditional microsphere measurements.

Materials and Methods

Mice

C57BL/6J male mice were purchased from Jackson Laboratory (Bar Harbor, ME, USA). Mice were provided standard chow and water *ad libitum*. They were housed 1–4 per cage in a room with a 12 hour light cycle. Cages contained corn cob bedding except during surgical recovery where iso pad bedding (Envigo, Indianapolis, Indiana, USA) was used until mice were ambulating normally. The Institutional Animal Care and Use Committee of the University of Virginia approved all animal experiments (#4116).

Mouse model of hindlimb ischemia

10–12 week old mice were anesthetized with ketamine (90 mg/kg) and xylazine (10 mg/kg). The left medial leg was shaved, depilated, and the area was prepared for aseptic surgery. Mice were kept under a heating lamp to maintain body temperature. An incision was made in the thigh to expose the femoral artery. 6–0 silk sutures were used to ligate the femoral artery proximal to the lateral circumflex femoral artery (Kochi et al. 2013). Care was taken to not damage major nerves or veins. Buprenorphine-SR (0.5 mg/kg) was administered after surgery and as needed in subsequent days. A total of 19 mice underwent hindlimb surgery for the serial studies by LDPI and CEUS, but 2 were lost due to complications of surgery. This left a total of 17 mice in which LDPI and CEUS were compared over time as described below. Ten of these 17 mice were used in a short-term serial comparison that was terminated at 14 days post-surgery. The other 7 mice were used in the long-term serial comparison that extended out to 150 days post-surgery.

Laser Doppler perfusion imaging (LDPI)

Mice were anesthetized with 1–2% isoflurane in oxygen and calves were shaved and depilated. Mice were placed prone under the LDPI instrument with legs extended and feet secured in place. The LDPI instrument employed in these studies was the PeriCam PSI (Perimed, Sweden), which has a resolution of 33 um/pixel and is widely used to assess perfusion in mouse models of HLI (Grau-Monge et al. 2017; Ma et al. 2021; Neale et al. 2020). Three to five measurements were taken, about one minute apart. Data were analyzed using the included PimSoft analysis software. ROIs were selected around the feet (below the ankle) or calves (between the knee and the ankle), the image intensity was averaged over all measurements, and a ratio of left:right (ischemic:control) foot was calculated.

Microbubble (MB) preparation

Microbubbles were prepared from decafluorobutane gas, which was dispersed in normal saline by sonication, essentially as described earlier (Unnikrishnan et al. 2018). Microbubbles were stabilized with a lipid monolayer shell that consisted of 1,2-distearoyl-*sn*-glycero-3-phosphocholine (DSPC) and PEG stearate. The microbubble population was floated at normal gravity to minimize microbubbles greater than 7 μm. Microbubbles of different sizes float at different rates, thus allowing for size separation (Connolly et al. 2014; Kvåle et al. 1996). Larger microbubbles were eliminated to ensure that none would get trapped in the lungs.

As shown in Fig 1, under the experimental conditions described here, a linear relationship between MB image intensity and MB concentration can be maintained by infusing up to 1×10^7 MB/min at a concentration of 1×10^9 MB/ml. Because the concentration of MBs in high concentration stocks declines with time during storage at 4C, the MB concentration in the stock solution was measured at least once every two weeks using a Coulter Counter (Beckman Coulter, Indianapolis, Indiana, USA). Based on that concentration, the microbubble stock was diluted to 1×10^9 MB/ml with sterile saline immediately prior to infusion at 10 μl/min.

Contrast enhanced ultrasound (CEUS)

Imaging was performed with an Acuson Sequoia C512 system and a 15L8W transducer (Siemens, Munich, Germany). Some groups have reported a transient increase in perfusion caused by ultrasound (Belcik et al. 2017). While we did not observe any increase in perfusion over the course of imaging, CEUS measurement were taken after LDPI measurements. Mice were anesthetized with 1–2% isoflurane in air rather than oxygen since the use of air as the carrier gas has been shown to increase the circulation lifetime of MB contrast agents (Mullin et al. 2011). A catheter with a 27G needle at the end was filled with heparinized saline (100 units/ml), inserted in the tail vein and secured. Mice were placed prone on a heated stage, legs extended, and feet secured. Ultrasound gel was placed on the calves and the transducer was oriented perpendicular across both calves and positioned mid-calf, taking care to maintain the same focal length and orientation each time. Scanning parameters were optimized and held constant as follows: frequency was 7 MHz, dynamic range was 100 dB, gain was −10 dB, imaging mechanical index was 0.2, burst mechanical index was 1.9, and burst time was one second. Using these settings, the resolution was measured to be 0.3 mm lateral and 0.2 mm axial. Video of the ultrasound exam was acquired in real time. Several B-mode frames were acquired before switching to contrast imaging mode. Microbubble solution was infused through the tail vein catheter at 1×10^7 MB/min (1×10^9 MB/ml MB solution concentration infused at 10 μl/min). During imaging, the syringe was rotated approximately every 30 seconds to prevent the microbubbles from floating and changing the concentration being infused. Pilot studies determined that steady state MB concentration was achieved within 5 minutes after the start of the infusion. The maintenance of steady state MB concentration was confirmed in each mouse by comparing imaging intensity over multiple burst-refresh cycles as illustrated in Figs 2B&C. Towards this end, high mechanical index burst pulses were applied once per minute for 10–15 minutes. The high mechanical index pulses cause the microbubbles in the field of view to

burst; while microbubbles from upstream continue to flow into the scanning plane, thus enabling perfusion to be quantified (Wei et al. 1998).

Video data were analyzed using a custom MATLAB (Mathworks, Natick, Massachusetts, USA) script. B-mode images were segmented to define ROIs for the left and right limbs. Image intensity over time was calculated and each flash-replenishment sequence was separated to allow for curve fitting. The first value after the high mechanical index pulse was taken as the background and subtracted out for each individual sequence. This also removes undue influence from any major arteries present in the ROI with very fast flow because the signal is already present in the first frame. The data were fit to $y=A*(1-e^{-\beta t})$ where A represents blood volume, β represents blood velocity and A*β represents blood flow (Wei et al. 1998). After reaching steady state, the four sequences with the lowest root mean square error were averaged to calculate A*β at each timepoint. This method of data sampling was adopted to simplify statistical analysis since a variable number of sequences (8–15) were collected at each time point. The average left:right (ischemic:control) A*β ratio was calculated for direct comparison with LDPI.

Fluorescent microspheres

Microspheres were sonicated no more than 24 hours prior to administration and were vortexed immediately before administration. Mice were anesthetized with pentobarbital (75 mg/kg) and intubated at 100 breaths/minute. The chest was opened and 200,000 green fluorescent microspheres (15 μm in diameter, Invitrogen, Carlsbad, California, USA) were injected into the left ventricle over two minutes (Serrat 2009). The microspheres were allowed to circulate for five minutes. Skeletal muscle on both limbs from just below the knee to just above the ankle was harvested and the bones were removed. Both kidneys were also harvested for reference purposes. Each tissue was blotted dry, weighed, and placed in a vial with a known amount of liquid and homogenized with a handheld, electric tissue homogenizer. Samples of homogenate from each tissue piece were placed on slides and sealed with a coverslip. The number of microspheres was counted on a fluorescence microscope (Olympus BX41, Olympus, Tokyo, Japan) and converted into units of spheres/g tissue to standardize a ratio of the left to right limb (ischemic:control) for comparison with LDPI and CEUS. Mice were excluded if there were less than 400 microspheres in the control limb, per the conventional 400 microsphere per sample rule (Buckberg et al. 1971), or if the kidneys were >15% different (Cardinal and Hoying 2007; Jädert et al. 2012), which is the conventional cutoff applied to avoid cases in which blood pool mixing was incomplete.

Tissue clearing and microscopy of in situ fluorescent microspheres

Muscle containing fluorescent microspheres was incubated in 4% paraformaldehyde at 4°C for 48–72 hours then rinsed three times with saline. A previously described CUBIC protocol was used for tissue clearing (Susaki et al. 2015). Incubation time was reduced as skeletal muscle clears significantly in just three days. Thin sections of muscle were teased apart, placed on slides, and sealed with a cover slip. Images were acquired on a fluorescence microscope (Olympus BX41, Olympus, Tokyo, Japan).

Histological analysis

Mice were anesthetized with ketamine (90 mg/kg) and xylazine (10 mg/kg), the chest was opened, and mice were perfused with heparinized saline (10 units/ml) followed by 4% paraformaldehyde. Both calves were harvested and incubated in paraformaldehyde at 4°C for 48–72 hours. Tissue was rinsed three times in saline and submerged in 15% sucrose overnight and then 30% sucrose overnight before flash freezing in OCT. 10 μm sections were cut and stained with hematoxylin and eosin (H&E).

Photoacoustic microscopy

Mice were anesthetized with 1–2% isoflurane and placed prone on a heated stage, legs extended, and feet secured. An incision was made in the skin along the gastrocnemius and the skin was secured so the muscle remained visible. Photoacoustic microscopy was performed as previously described (Ning et al. 2015). Briefly, a multi-parametric PAM platform used dual-wavelength photoacoustic excitation for imaging microvascular anatomy and oxygen saturation. In addition, blood flow was mapped by flow-induced temporal decorrelation.

Statistical analysis

All results are presented as mean±SEM. A linear mixed model with Bonferroni correction was used to analyze the longitudinal LDPI and CEUS data using SAS version 9.4 (SAS Institute, Inc., Cary, NC, USA). Comparisons between more than two groups were performed with a one-way ANOVA and post-hoc analysis (Tukey's test) as appropriate. $P<0.05$ was considered significant. Data were checked for normality using the Shapiro-Wilk test. Except as noted, GraphPad Prism version 5.0 (GraphPad Software, San Diego, CA, USA) was used to perform statistical analyses.

Results

CEUS is well suited for hindlimb perfusion assessments

By positioning the 5cm wide 15L8W transducer perpendicular to the long-axes of the two mouse hindlimbs, we were able to assess both calves simultaneously in a single imaging plane (Fig 1 and Video 1). Imaging and microbubble infusion parameters were optimized for this application, and the sensitivity for detecting perfusion defects was maximized by performing CEUS at a steady-state MB concentration that corresponded to the high-end of linear range in normally-perfused control muscle (see Fig 1). To evaluate variability within and between mice, four mice that had not undergone surgery were assessed for left:right perfusion ratio on four successive days with CEUS (Fig 2). As anticipated, unoperated mice exhibited modest variability in left:right perfusion ratios on successive days, comparable with the variability reported in human subjects (Marcinkevics et al. 2013; Mayrovitz and Larsen 1996). However, repeated perfusion measurements taken during a single imaging session exhibited minimal variability.

CEUS and LDPI show different perfusion recoveries over time

To compare perfusion recovery as measured by LDPI and CEUS, mice were imaged by both techniques before surgery, and on days 1, 4, 7, 14, 28, 60, 90, and 150 after surgery (Fig 3, Video 2, and Video 3). A group of ten mice were serially imaged by LDPI and CEUS for 14 days after surgery, and a separate group of seven mice were serially imaged by LDPI and CEUS for 150 days after surgery. Perfusion ratios by LDPI and CEUS were significantly different at every time point except day 4 post-surgery. Day one post-surgery, perfusion in the ischemic limb as measured by LDPI was reduced to 72±1% of the control limb. Perfusion in the ischemic limb then increased until day 14 post-surgery, at which time it returned to pre-surgery levels and remained steady until day 150 post-surgery. By CEUS, day one post-surgery perfusion in the ischemic limb was reduced to 25±1% of the control limb. In contrast to LDPI, perfusion by CEUS then increased until day 4 post-surgery when it reached a peak of 77±2% of the control limb and remained similar at day 7 post-surgery at 69±1% of the control limb. A modest decline was noted by CEUS from day 7 to day 14 post-surgery, but perfusion in the ischemic limb leveled off to an average of 56% of the control limb for the duration of the study (until 150 days post-surgery). Since there were small differences between LDPI and CEUS perfusion ratios before surgery, the data were also analyzed as a change from the pre-surgery perfusion ratios. By LDPI, perfusion returned to normal by day 28 post-surgery ($p=0.667$); but by CEUS, perfusion in the ischemic limb never returned to normal ($p<0.001$). To ensure the transducer was performing uniformly along its length, we used a hydrophone to measure the output across three points on the transducer, no differences were seen. Additionally, an *in vivo* assessment of the transducer was performed. A mouse was imaged using the transducer orientation in these studies, and halfway through the transducer was turned 180°. Both orientations resulted in the same perfusion ratio.

Since LDPI measurements in hindlimb ischemia studies are almost always taken in the feet, we chose to use those measurements to compare with CEUS. However, to address this disparity, measurements in the calves by LDPI were also performed before surgery and days 1, 4, 7, and 14 after surgery (Fig 4). Before surgery, the perfusion ratio in the calves was 1.09±0.03 vs 1.01±0.03 in the feet. Day one post-surgery, perfusion in the ischemic calf was greater than in the foot, 0.84±0.05 vs 0.72±0.03. Perfusion recovery was faster in the calves than the feet, corresponding to the lesser initial reduction in perfusion. Overall perfusion recovery trends by LDPI in the calves mimic those in the feet, and when compared to the CEUS calf results, the difference in the two techniques remains.

Fluorescent microspheres show impaired perfusion

As the results from LDPI and CEUS differed significantly, relative perfusion between limbs was additionally assessed by fluorescent microspheres, the conventional standard for perfusion measurements in large animals. Perfusion by LDPI, CEUS, and fluorescent microspheres were compared at day 14 post-surgery (Fig 5). LDPI showed a normal perfusion ratio (0.9±0.1) which was significantly different than both CEUS (0.5±0.1) and fluorescent microspheres (0.6±0.2). CEUS and fluorescent microspheres were not significantly different, both suggesting that perfusion never returns to normal in mice subjected to hindlimb ischemia.

Pathological muscle morphology and function

Muscle morphology in control and ischemic limbs was evaluated with H&E staining day 150 post-surgery (Fig 6). Muscle from the ischemic limbs showed irregular fibers and many fibers with centralized nuclei. In control limbs, the majority of muscle fibers had peripheral nuclei and there was a more consistent fiber architecture. Photoacoustic microscopy was used to evaluate oxygen saturation, perfusion, and vascular structure before HLI and 14 days post-surgery in gastrocnemius muscle (Fig 7). Results indicated that oxygen saturation and perfusion remain reduced 14 days post-surgery, consistent with recent reports (Arpino et al. 2017). Anatomically, the vasculature in the ischemic limb was irregular and tortuous, and there were very few larger vessels evident.

Discussion

In this study, we sought to evaluate perfusion measurement techniques in a mouse model of hindlimb ischemia. The three techniques utilized were LDPI, CEUS, and fluorescent microspheres. CEUS was shown to be well suited for hindlimb perfusion assessments. Variability in CEUS-derived perfusion ratios within and between mice, while greater than LDPI, is consistent with the variability in clinical perfusion values reported in human subjects (Marcinkevics et al. 2013; Mayrovitz and Larsen 1996). In mice, CEUS enabled measurements of a cross-sectional view of both calves simultaneously, allowing for an internal control.

Since LDPI is the most common measurement method employed in mouse HLI models, we next performed a direct comparison between CEUS and LDPI over a 150 day time course following the surgical induction of HLI. The LDPI perfusion recovery results are consistent with other reports from similar surgical procedures over the course of several decades (Couffinhal et al. 1998; Helisch et al. 2006; Hellingman et al. 2010; Stabile et al. 2003; Waters et al. 2004). Interestingly, left to right perfusion ratios in the calves were above one at baseline prior to surgery, both as assessed by CEUS (1.16±0.09) and LDPI (1.09 ±0.03). Subsequent quality control studies indicated that this was not attributable to a defect in CEUS instrumentation or procedures, leaving open the possibility of an underlying biological difference between hindlimbs. For example, a mean difference in human limb perfusion of 10%, as measured by MRI flowmetry, was reported by Mayrovitz and Larsen (Mayrovitz and Larsen 1996). Given the difference at baseline, the data were also analyzed as a function of change from the pre-surgery perfusion ratios. To our surprise, we found that CEUS and LDPI show very different perfusion recovery kinetics and outcomes. The techniques differed at nearly every time point, although they did portray broadly similar trends in recovery during the first week following surgery. This was true for both comparisons of LDPI in the calves and feet to CEUS in the calves.

Some of these differences can be explained by the techniques themselves. It might be expected that the skin (LDPI) and muscle (CEUS) would recover at different rates. These are different vascular beds with different metabolic needs and, in some cases, different feeding arteries. The similar trends in perfusion recovery by LDPI and CEUS during the first week of surgery are consistent with this possibility. However, it is unexpected and striking that mice never fully recover perfusion in the ischemic hindlimb when assessed by

CEUS, and we validated this finding using a completely independent method (fluorescent microspheres). Given the destructive nature of the fluorescent microsphere measurement, the sample size was limited and serial assessments were not possible. Despite this limitation, these results are also supported by a recent study by Arpino and colleagues. They used intravital microscopy to probe arterial morphology and function after HLI in the extensor digitorum longus muscle, and their results are consistent with our findings, showing incomplete recovery up to 120 days post-surgery (Arpino et al. 2017).

The independent data from histopathology and photoacoustic microscopy provide additional support by demonstrating abnormal muscle morphology and lower oxygenation and perfusion levels. Several other studies also document abnormal muscle morphology by histology at various time points that is consistent with our results showing irregular myofibers and centralized nuclei (Arpino et al. 2017; Brenes et al. 2012; Lian et al. 2010). This has significant implications for the field, because it suggests that LDPI results (which measures perfusion in skin and superficial muscle) may not accurately represent perfusion in the deeper muscle of the calves, though the assumption has been that measurements in the feet are reflective of limb perfusion. This may partially explain some of the difficulties in translating preclinical successes to the clinic since the majority of vessels supplying the muscle, and the primary sites of atherosclerosis and vessel occlusion in PAD, are deeper in the calf and thigh muscle.

In the CEUS results, we observed an unexpected peak in the perfusion ratios on days 4 and 7 post-surgery. Based on previously studies employing LDPI, we had expected to see a nearly linear recovery in perfusion over time. A potential explanation for the unexpected peak is that, after the induction of ischemia, there is overgrowth and subsequent pruning of the vasculature coinciding with the increase and the decrease in perfusion. This was shown to occur by Landázuri and colleagues in a mouse model of hindlimb ischemia where the femoral artery and vein were ligated and excised (Landázuri et al. 2012). Using micro-CT this group showed that vascular volume, density, and connectivity peak at day 7 post-surgery and then decline.

Importantly, our findings suggest a more physiologically relevant model for testing therapeutic approaches to PAD. When using traditional LDPI, therapies are considered successful if they accelerate perfusion recovery since LDPI indicates that mice regain normal perfusion within a few weeks, even without any treatment. This is not at all representative of what happens in PAD patients, who experience a chronic and often declining disease state. Ironically, this study adds to the accumulating evidence to suggest that the mouse HLI model of PAD is actually quite faithful to the human disease process. When assessed by CEUS, this same mouse model appears to offer a more physiologically relevant test bed where mice reach a plateau in perfusion recovery that is more similar to reported patient outcomes (Stoyioglou and Jaff 2004). We propose a new approach to evaluating therapies, where HLI surgery is performed, mice are allowed to reach a perfusion plateau, and then a therapeutic intervention is applied and assessed by CEUS. This method more accurately models the clinical condition and would allow for testing of therapies for their ability to improve perfusion long term, rather than just accelerate perfusion recovery.

To our knowledge, this is the first study to provide a serial comparison of LDPI and CEUS over an extended time course, as well as the first study to show a persistent perfusion deficit by CEUS in a mouse model of hindlimb ischemia. We believe this may also be the first study to use repeated, label-free photoacoustic microscopy in a mouse model of HLI, although Ye and colleagues previously reported photoacoustic microscopy imaging at much lower resolution (and without oxygen saturation mapping) in a mouse model of HLI (Ye et al. 2012).

There are several limitations of this work that must be considered. One major limitation is the small number of microsphere measurements that were able to be performed. Ideally microsphere measurements would have been taken at several timepoints, however given their destructive nature we chose what we believed would be the most useful timepoint to have that data. Another limitation is the CEUS data was collected in one imaging plane, with the assumption that the calf perfusion would be relatively consistent regardless of the level of measurement. We evaluated different planes in normal mice and those measurements were consistent with each other, however there is a possibility that after induction of hindlimb ischemia that assumption would not hold true. Finally, it is possible that CEUS imaging itself altered the perfusion recovery in these mice. Contrast ultrasound is known to cause bioeffects, though the ultrasound settings used in this application are unlikely to cause them. Any effect would probably be caused by the high MI burst pulse, but the burst pulse was brief compared to studies that report negative bioeffects (ter Haar 2010). Given the similarity of recovery by LDPI and results reported in the literature we do not believe to be likely that CEUS altered perfusion recovery.

The use of CEUS to measure limb perfusion is not limited to animal research applications (Bajwa et al. 2014; Nguyen and Davidson 2019). There are several groups that have used CEUS in humans to evaluate PAD (Kundi et al. 2017; Lindner et al. 2008). Rather than the ratiometric assay used in preclinical studies where the unaffected limb serves as an internal control, clinical studies typically compare perfusion parameters before and after exercise stress (Davidson et al. 2017). These studies have shown a significant differences between normal and PAD patients (Kundi et al. 2017; Lindner et al. 2008). The successful use of CEUS in the clinical evaluation of PAD provides further confidence in the value of this technique in preclinical research.

Conclusions

In summary, this study aimed to evaluate perfusion measurement techniques used in mouse models of HLI. We showed that, despite being the most commonly used technique, the use of LDPI for perfusion measurements in a PAD model yields results that are inconsistent with CEUS, microsphere measurements, histopathology, photoacoustic microscopy, as well as clinical outcomes in PAD patients. These results provide a potential explanation for why the vast majority of therapies developed in the mouse HLI model ultimately fail in clinical trials, and suggest a new path forward for preclinical evaluation of therapeutics for the treatment of PAD.

Supplementary Material

Refer to Web version on PubMed Central for supplementary material.

Acknowledgements

The authors would like to thank R. John Lye and Vijay C. Ganta for their help and advice in mouse HLI models of PAD. We would also like to thank Jim Patrie, M.S. in the UVA Department of Public Health Sciences for his contribution to the statistical analysis of the time course of recovery data set. This work was supported by American Heart Association Grant #15PRE25100003 (Alyssa B. Becker) and NIH/NHLBI grant R01HL116455 (MPI to Brian H. Annex and Brent A. French).

References

Aref Z, de Vries MR, Quax PHA. Variations in Surgical Procedures for Inducing Hind Limb Ischemia in Mice and the Impact of These Variations on Neovascularization Assessment. Int J Mol Sci 2019;20:3704. [PubMed: 31362356]

Arpino JM, Nong Z, Li F, Yin H, Ghonaim N, Milkovich S, Balint B, O'Neil C, Fraser GM, Goldman D, Ellis CG, Pickering JG. Four-Dimensional Microvascular Analysis Reveals That Regenerative Angiogenesis in Ischemic Muscle Produces a Flawed Microcirculation. Circ Res 2017;120:1453–1465. [PubMed: 28174322]

Bajwa A, Wesolowski R, Patel A, Saha P, Ludwinski F, Smith A, Nagel E, Modarai B. Assessment of Tissue Perfusion in the Lower Limb. Circ Cardiovasc Imaging 2014;7:836–843. [PubMed: 25227236]

Baltgalvis KA, White K, Li W, Claypool MD, Lang W, Alcantara R, Singh BK, Friera AM, McLaughlin J, Hansen D, McCaughey K, Nguyen H, Smith IJ, Godinez G, Shaw SJ, Goff D, Singh R, Markovtsov V, Sun T-Q, Jenkins Y, Uy G, Li Y, Pan A, Gururaja T, Lau D, Park G, Hitoshi Y, Payan DG, Kinsella TM. Exercise performance and peripheral vascular insufficiency improve with AMPK activation in high-fat diet-fed mice. Am J Physiol-Heart Circ Physiol 2014;306:H1128–H1145. [PubMed: 24561866]

Baron DM, Clerte M, Brouckaert P, Raher MJ, Flynn AW, Zhang H, Carter EA, Picard MH, Bloch KD, Buys ES, Scherrer-Crosbie M. In Vivo Noninvasive Characterization of Brown Adipose Tissue Blood Flow by Contrast Ultrasound in Mice. Circ Cardiovasc Imaging 2012;5:652–659. [PubMed: 22776888]

Belcik JT, Davidson BP, Xie A, Wu MD, Yadava M, Qi Y, Liang S, Chon CR, Ammi AY, Field J, Harmann L, Chilian WM, Linden J, Lindner JR. Augmentation of Muscle Blood Flow by Ultrasound Cavitation Is Mediated by ATP and Purinergic Signaling. Circulation American Heart Association, 2017;135:1240–1252.

Brenes RA, Jadlowiec CC, Bear M, Hashim P, Protack CD, Li X, Lv W, Collins MJ, Dardik A. Toward a mouse model of hind limb ischemia to test therapeutic angiogenesis. J Vasc Surg 2012;56:1669–1679. [PubMed: 22836102]

Briers JD. Laser Doppler, speckle and related techniques for blood perfusion mapping and imaging. Physiol Meas 2001;22:R35–R66. [PubMed: 11761081]

Buckberg GD, Luck JC, Payne DB, Hoffman JI, Archie JP, Fixler DE. Some sources of error in measuring regional blood flow with radioactive microspheres. J Appl Physiol 1971;31:598–604. [PubMed: 5111009]

Cao WJ, Rosenblat JD, Roth NC, Kuliszewski MA, Matkar PN, Rudenko D, Liao C, Lee PJH, Leong-Poi H. Therapeutic Angiogenesis by Ultrasound-Mediated MicroRNA-126–3p Delivery. Arterioscler Thromb Vasc Biol American Heart Association, 2015;35:2401–2411.

Cardinal TR, Hoying JB. A modified fluorescent microsphere-based approach for determining resting and hyperemic blood flows in individual murine skeletal muscles. Vascul Pharmacol 2007;47:48–56. [PubMed: 17500044]

Connolly F, Rae MT, Butler M, Klibanov AL, Sboros V, McNeilly AS, Duncan WC. The Local Effects of Ovarian Diathermy in an Ovine Model of Polycystic Ovary Syndrome. PLOS ONE Public Library of Science, 2014;9:e111280.

Couffinhal T, Silver M, Zheng LP, Kearney M, Witzenbichler B, Isner JM. Mouse model of angiogenesis. Am J Pathol 1998;152:1667–1679. [PubMed: 9626071]

Davidson BP, Belcik JT, Landry G, Linden J, Lindner JR. Exercise versus vasodilator stress limb perfusion imaging for the assessment of peripheral artery disease. Echocardiogr Mt Kisco N 2017;34:1187–1194.

Davis MA, Kazmi SMS, Dunn AK. Imaging depth and multiple scattering in laser speckle contrast imaging. J Biomed Opt 2014 [cited 2019 Jan 4];19. Available from: https://www.ncbi.nlm.nih.gov/pmc/articles/PMC4119427/

Fowkes FGR, Rudan D, Rudan I, Aboyans V, Denenberg JO, McDermott MM, Norman PE, Sampson UK, Williams LJ, Mensah GA, Criqui MH. Comparison of global estimates of prevalence and risk factors for peripheral artery disease in 2000 and 2010: a systematic review and analysis. The Lancet 2013;382:1329–1340.

French BA, Li Y, Klibanov AL, Yang Z, Hossack JA. 3D perfusion mapping in post-infarct mice using myocardial contrast echocardiography. Ultrasound Med Biol 2006;32:805–815. [PubMed: 16785003]

Grau-Monge C, Delcroix GJ-R, Bonnin-Marquez A, Valdes M, Awadallah ELM, Quevedo DF, Armour MR, Montero RB, Schiller PC, Andreopoulos FM, D'Ippolito G. MIAMI cells embedded within a biologically-inspired construct promote recovery in a mouse model of peripheral vascular disease. Biomed Mater Bristol Engl 2017;12:015024.

Haar G ter. Ultrasound bioeffects and safety. Proc Inst Mech Eng [H] IMECHE, 2010;224:363–373.

Halpern EJ. Contrast-Enhanced Ultrasound Imaging of Prostate Cancer. Rev Urol 2006;8:S29–S37. [PubMed: 17021624]

Helisch A, Wagner S, Khan N, Drinane M, Wolfram S, Heil M, Ziegelhoeffer T, Brandt U, Pearlman JD, Swartz HM, Schaper W. Impact of Mouse Strain Differences in Innate Hindlimb Collateral Vasculature. Arterioscler Thromb Vasc Biol 2006;26:520–526. [PubMed: 16397137]

Hellingman AA, Bastiaansen AJNM, de Vries MR, Seghers L, Lijkwan MA, Löwik CW, Hamming JF, Quax PHA. Variations in Surgical Procedures for Hind Limb Ischaemia Mouse Models Result in differences in Collateral Formation. Eur J Vasc Endovasc Surg 2010;40:796–803. [PubMed: 20705493]

Iyer SR, Annex BH. Therapeutic Angiogenesis for Peripheral Artery Disease. JACC Basic Transl Sci 2017;2:503–512. [PubMed: 29430558]

Jädert C, Petersson J, Massena S, Ahl D, Grapensparr L, Holm L, Lundberg JO, Phillipson M. Decreased leukocyte recruitment by inorganic nitrate and nitrite in microvascular inflammation and NSAID-induced intestinal injury. Free Radic Biol Med 2012;52:683–692. [PubMed: 22178413]

Karvinen H, Pasanen E, Rissanen TT, Korpisalo P, Vähäkangas E, Jazwa A, Giacca M, Ylä-Herttuala S. Long-term VEGF-A expression promotes aberrant angiogenesis and fibrosis in skeletal muscle. Gene Ther 2011;18:1166–1172. [PubMed: 21562595]

Klibanov AL. Ultrasound Contrast Materials in Cardiovascular Medicine: from Perfusion Assessment to Molecular Imaging. J Cardiovasc Transl Res 2013;6:10.1007/s12265-013-9501-0.

Kochi T, Imai Y, Takeda A, Watanabe Y, Mori S, Tachi M, Kodama T. Characterization of the Arterial Anatomy of the Murine Hindlimb: Functional Role in the Design and Understanding of Ischemia Models. PLOS ONE 2013;8:e84047. [PubMed: 24386328]

Krishna SM, Omer SM, Golledge J. Evaluation of the clinical relevance and limitations of current pre-clinical models of peripheral artery disease. Clin Sci 2016;130:127–150.

Krix M, Weber M-A, Krakowski-Roosen H, Huttner HB, Delorme S, Kauczor H-U, Hildebrandt W. Assessment of Skeletal Muscle Perfusion Using Contrast-Enhanced Ultrasonography. J Ultrasound Med 2005;24:431–441. [PubMed: 15784761]

Kuliszewski MA, Kobulnik J, Lindner JR, Stewart DJ, Leong-Poi H. Vascular Gene Transfer of SDF-1 Promotes Endothelial Progenitor Cell Engraftment and Enhances Angiogenesis in Ischemic Muscle. Mol Ther 2011;19:895–902. [PubMed: 21364544]

Kundi R, Prior SJ, Addison O, Lu M, Ryan AS, Lal BK. Contrast-Enhanced Ultrasound Reveals Exercise-Induced Perfusion Deficits in Claudicants. J Vasc Endovasc Surg 2017 [cited 2019 Apr 14];2. Available from: https://www.ncbi.nlm.nih.gov/pmc/articles/PMC5501290/

Kvåle S, Jakobsen HA, Asbjørnsen OA, Omtveit T. Size fractionation of gas-filled microspheres by flotation. Sep Technol 1996;6:219–226.

Landázuri N, Joseph G, Guldberg RE, Taylor WR. Growth and regression of vasculature in healthy and diabetic mice after hindlimb ischemia. Am J Physiol - Regul Integr Comp Physiol 2012;303:R48–R56. [PubMed: 22573106]

Leong-Poi H, Christiansen J, Heppner P, Lewis CW, Klibanov AL, Kaul S, Lindner JR. Assessment of Endogenous and Therapeutic Arteriogenesis by Contrast Ultrasound Molecular Imaging of Integrin Expression. Circulation American Heart Association, 2005;111:3248–3254.

Leyba KA, Vasudevan S, O'Sullivan TD, Goergen CJ. Evaluation of Hemodynamics in a Murine Hindlimb Ischemia Model Using Spatial Frequency Domain Imaging. Lasers Surg Med 2021;53:557–566. [PubMed: 32956499]

Lian Q, Zhang Y, Zhang J, Zhang H, Wu X, Zhang Y, Lam FF-Y, Kang S, Xia JC, Lai W, Au KTP, Chow YY, Siu CD, Lee C, Tse H. Functional mesenchymal stem cells derived from human induced pluripotent stem cells attenuate limb ischemia in mice. Circulation 2010;121:1113–1123. [PubMed: 20176987]

Lindner JR, Womack L, Barrett EJ, Feltman J, Price W, Harthun NL, Kaul S, Patrie JT. Limb Stress-Rest Perfusion Imaging With Contrast Ultrasound For The Assessment Of Peripheral Arterial Disease Severity. JACC Cardiovasc Imaging 2008;1:343–350. [PubMed: 19356447]

Ma Y, Jia L, Wang Y, Ji Y, Chen J, Ma H, Lin X, Zhang Y, Li W, Ni H, Xie L, Xie Y, Xiang M. Heme Oxygenase-1 in Macrophages Impairs the Perfusion Recovery After Hindlimb Ischemia by Suppressing Autolysosome-Dependent Degradation of NLRP3. Arterioscler Thromb Vasc Biol American Heart Association, 2021;41:1710–1723.

Marcinkevics Z, Lukstina Z, Rubins U, Grabovskis A, Aivars J-I. Bilateral difference of superficial and deep femoral artery haemodynamic and anatomical parameters. Artery Res 2013;7:201–210.

Mayrovitz HN, Larsen PB. Pulsatile blood flow asymmetry in paired human legs. Clin Physiol 1996;16:495–505. [PubMed: 8889313]

Mullin L, Gessner R, Kwan J, Kaya M, Borden MA, Dayton PA. Effect of Anesthesia Carrier Gas on In-Vivo Circulation Times of Ultrasound Microbubble Contrast Agents in Rats. Contrast Media Mol Imaging 2011;6:126–131. [PubMed: 21246710]

Neale JPH, Pearson JT, Thomas KN, Tsuchimochi H, Hosoda H, Kojima M, Sato T, Jones GT, Denny AP, Daniels LJ, Chandrasekera D, Liu P, van Rij AM, Katare R, Schwenke DO. Dysregulation of ghrelin in diabetes impairs the vascular reparative response to hindlimb ischemia in a mouse model; clinical relevance to peripheral artery disease. Sci Rep 2020;10:13651. [PubMed: 32788622]

Nguyen T, Davidson BP. Contrast Enhanced Ultrasound Perfusion Imaging in Skeletal Muscle. J Cardiovasc Imaging 2019 [cited 2019 Jun 5];27. Available from: 10.4250/jcvi.2019.27.e31

Ning B, Kennedy MJ, Dixon AJ, Sun N, Cao R, Soetikno BT, Chen R, Zhou Q, Shung KK, Hossack JA, Hu S. Simultaneous photoacoustic microscopy of microvascular anatomy, oxygen saturation, and blood flow. Opt Lett 2015;40:910–913. [PubMed: 25768144]

Ouriel K Peripheral arterial disease. The Lancet 2001;358:1257–1264.

Prinzen F Blood flow distributions by microsphere deposition methods. Cardiovasc Res 2000;45:13–21. [PubMed: 10728307]

Pysz MA, Foygel K, Panje CM, Needles A, Tian L, Willmann JK. Assessment and Monitoring Tumor Vascularity With Contrast-Enhanced Ultrasound Maximum Intensity Persistence Imaging. Invest Radiol 2011;46:187–195. [PubMed: 21150790]

Rissanen TT, Korpisalo P, Karvinen H, Liimatainen T, Laidinen S, Gröhn OH, Ylä-Herttuala S. High-Resolution Ultrasound Perfusion Imaging of Therapeutic Angiogenesis. JACC Cardiovasc Imaging 2008;1:83–91. [PubMed: 19356410]

Rollins AM, Yazdanfar S, Barton JK, Izatt JA. Real-time in vivo color Doppler optical coherence tomography. J Biomed Opt SPIE, 2002;7:123–129.

Ryu JC, Davidson BP, Xie A, Qi Y, Zha D, Belcik JT, Caplan ES, Woda JM, Hedrick CC, Hanna RN, Lehman N, Zhao Y, Ting A, Lindner JR. Molecular Imaging of the Paracrine Proangiogenic Effects of Progenitor Cell Therapy in Limb Ischemia. Circulation American Heart Association, 2013;127:710–719.

Schinkel AFL, Kaspar M, Staub D. Contrast-enhanced ultrasound: clinical applications in patients with atherosclerosis. Int J Cardiovasc Imaging 2016;32:35–48. [PubMed: 26206524]

Senarathna J, Rege A, Li N, Thakor NV. Laser Speckle Contrast Imaging: Theory, Instrumentation and Applications. IEEE Rev Biomed Eng 2013;6:99–110. [PubMed: 23372086]

Serrat MA. Measuring bone blood supply in mice using fluorescent microspheres. Nat Protoc 2009;4:1749–1758.

Shuoqi Ye SY, Junyu Yang JY, Jianzhong Xi JX, Qiushi Ren QR, Changhui Li CL. Studying murine hindlimb ischemia by photoacoustic microscopy. Chin Opt Lett 2012;10:121701–121704.

Smith AH, Kuliszewski MA, Liao C, Rudenko D, Stewart DJ, Leong-Poi H. Sustained Improvement in Perfusion and Flow Reserve After Temporally Separated Delivery of Vascular Endothelial Growth Factor and Angiopoietin-1 Plasmid Deoxyribonucleic Acid. J Am Coll Cardiol 2012;59:1320–1328. [PubMed: 22464261]

Stabile E, Burnett MS, Watkins C, Kinnaird T, Bachis A, la Sala A, Miller JM, Shou M, Epstein SE, Fuchs S. Impaired Arteriogenic Response to Acute Hindlimb Ischemia in CD4-Knockout Mice. Circulation 2003;108:205–210. [PubMed: 12821542]

Stoyioglou A, Jaff MR. Medical Treatment of Peripheral Arterial Disease: A Comprehensive Review. J Vasc Interv Radiol 2004;15:1197–1207. [PubMed: 15525738]

Sullivan JC, Wang B, Boesen EI, D'Angelo G, Pollock JS, Pollock DM. Novel use of ultrasound to examine regional blood flow in the mouse kidney. Am J Physiol-Ren Physiol 2009;297:F228–F235.

Susaki EA, Tainaka K, Perrin D, Yukinaga H, Kuno A, Ueda HR. Advanced CUBIC protocols for whole-brain and whole-body clearing and imaging. Nat Protoc 2015;10:1709–1727. [PubMed: 26448360]

Unnikrishnan S, Du Z, Diakova GB, Klibanov AL. Formation of Microbubbles for Targeted Ultrasound Contrast Imaging: Practical Translation Considerations. Langmuir 2018 [cited 2019 May 14]; Available from: 10.1021/acs.langmuir.8b03551

Waters RE, Terjung RL, Peters KG, Annex BH. Preclinical models of human peripheral arterial occlusive disease: implications for investigation of therapeutic agents. J Appl Physiol 2004;97:773–780. [PubMed: 15107408]

Wei K, Jayaweera AR, Firoozan S, Linka A, Skyba DM, Kaul S. Quantification of Myocardial Blood Flow With Ultrasound-Induced Destruction of Microbubbles Administered as a Constant Venous Infusion. Circulation 1998;97:473–483. [PubMed: 9490243]

Shuoqi Ye, Junyu Yang, Jianzhong Xi, Qiushi Ren, Changhui Li. Studying murine hindlimb ischemia by photoacoustic microscopy. Chin Opt Lett 2012;10:121701–121704.

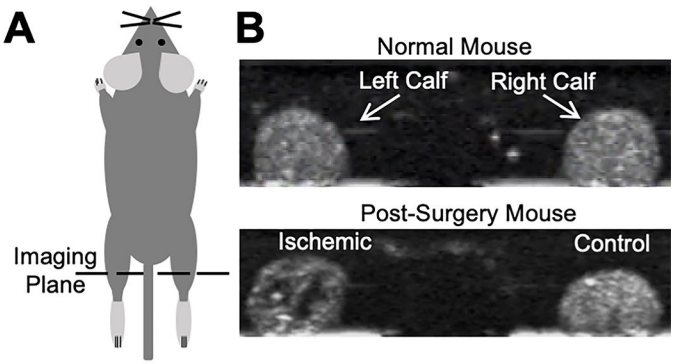

C

Variable	Range Tested	Selected Value
Frequency	7-12 MHz	7 MHz
Dynamic Range	55-100 dB	100 dB
Gain	-20-0	-10
Flash Replenishment Interval	20-60 s	60 s
Burst Time	1-2 s	1 s
MB Concentration	$1x10^8$-$1x10^9$ MB/ml	$1x10^9$ MB/ml
MB Infusion Rate	2.5-20 μl/min	10 μl/min

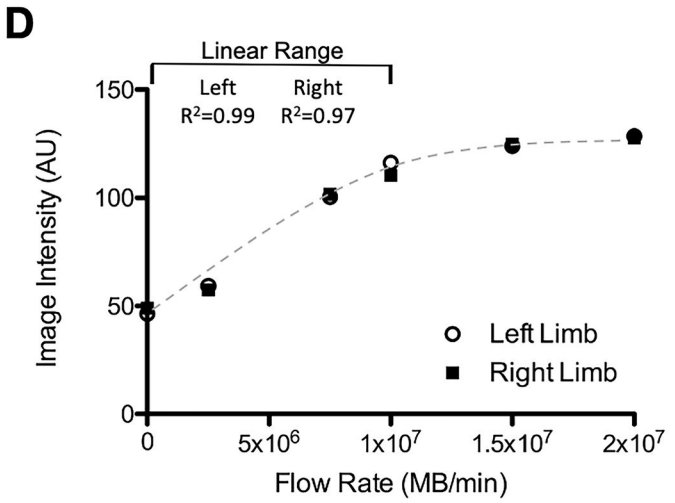

Fig 1. Set up and parameters for CEUS.

A) Schematic of transducer placement across both calves. B) Example CEUS images of calf cross sections in contrast mode with microbubbles in circulation in a normal mouse and a mouse that underwent HLI surgery. The ischemic limb in the post-surgery mouse shows reduced image intensity in areas with minimal flow. See supplemental material for videos of CEUS imaging. C) Tested and selected values for optimized ultrasound parameters. D) Image intensities in the left and right limbs over a range of microbubble flow rates show a linear range up to 1×10^7 MB/min.

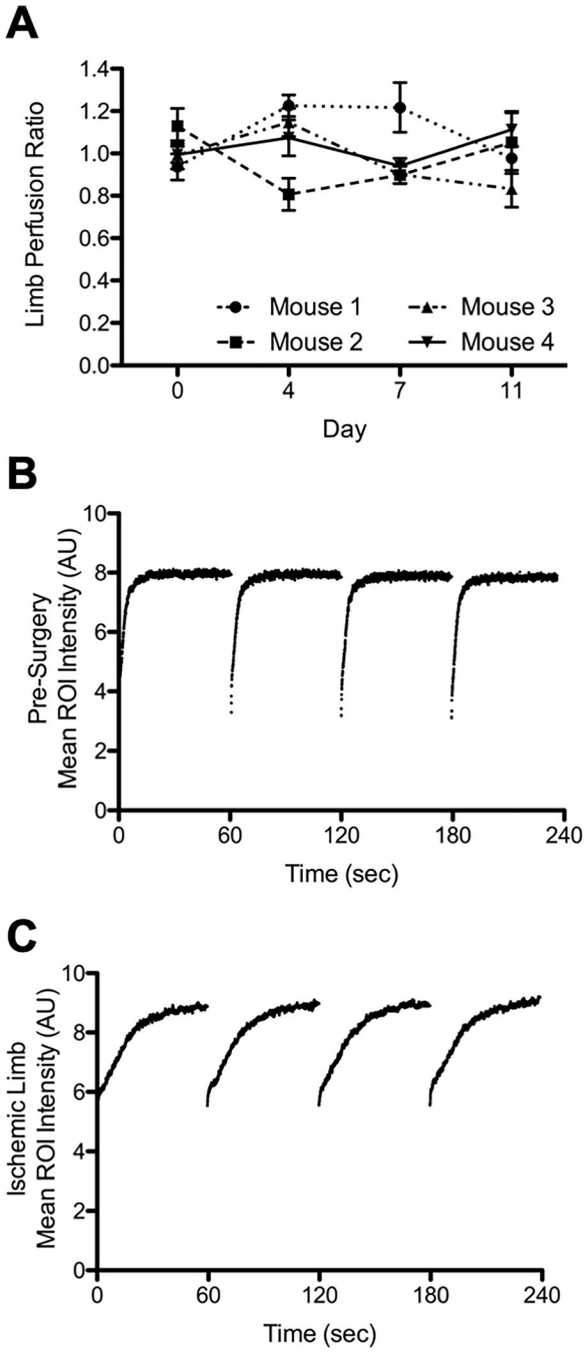

Fig 2. CEUS provides consistent perfusion measurements and clear distinctions between normal and abnormal perfusion.

A) Test-retest measurements of hindlimb blood perfusion ratios by CEUS. Perfusion ratios in four mice each measured four times over eleven days show modest variation over time. Measurements during a single imaging session showed minimal variation. B) Example of four contiguous sequences of flash-replenishment data from a normal limb. C) Example of four sequences of flash-replenishment data from a limb one day post-surgery shows a much slower rate of microbubble replenishment (recovery of intensity), indicating reduced perfusion.

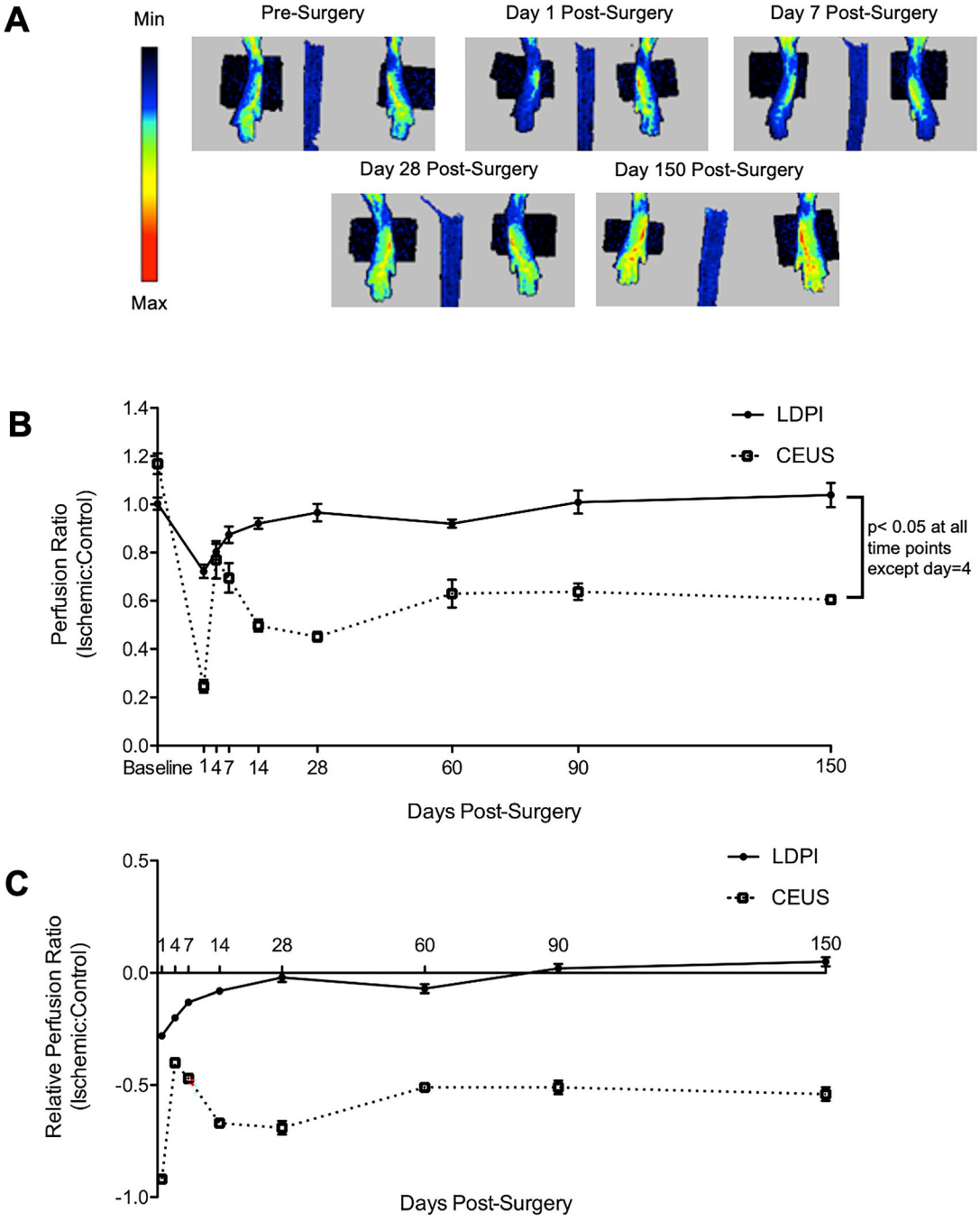

Fig 3. Perfusion recovery after HLI by LDPI shows full recovery by 28 days, CEUS shows perfusion never recovers.

A) Representative images of perfusion recovery measured by LDPI. B) The ratio of perfusion in ischemic:control limbs as measured by LDPI and CEUS at baseline and days 1, 4, 7, 14, 28, 60, 90, and 150 after surgery. By LDPI, perfusion returns to normal within 14 days post-surgery. However, by CEUS perfusion is more severely reduced at day 1, then improves modestly at days 4 and 7 before achieving a plateau at ~50% of the control limb through the end of the study. Measurements by LDPI and CEUS are significantly different at all time points except day 4 post-surgery ($p<0.05$; n=17 for pre-14 day time points, n=7

for 28–150 day time points). C) The ratio of perfusion in ischemic:control limbs relative to the pre-surgery perfusion ratios. By LDPI, perfusion is significantly reduced through day 14 post-surgery ($p<0.05$ vs. baseline), but returns to normal by day 28 post-surgery. In contrast, perfusion by CEUS remains persistently depressed for at least 150 days post-surgery ($p<0.001$ vs. baseline). Statistical analysis was performed using a linear mixed model with Bonferroni correction.

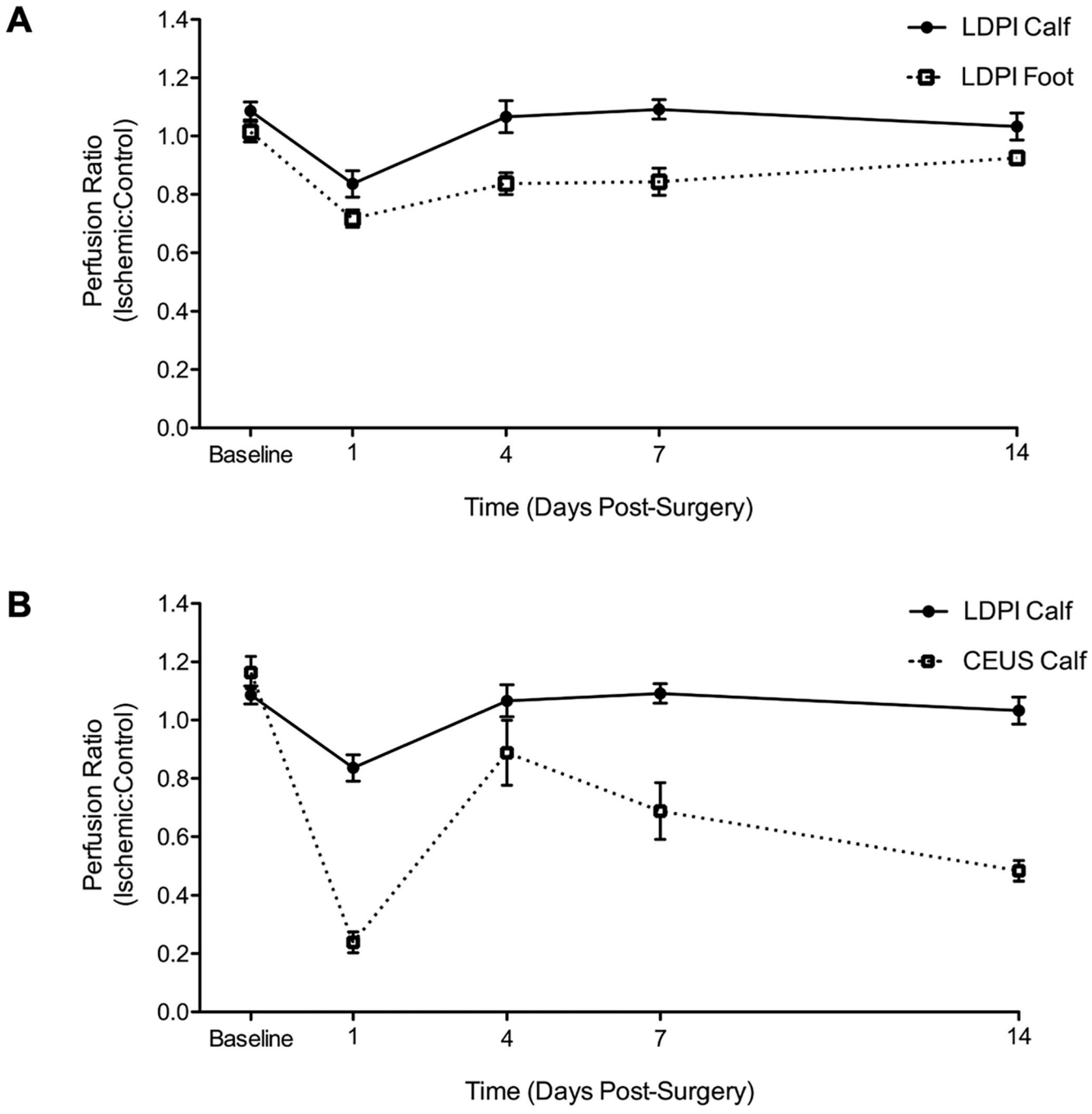

Fig 4. LDPI measurements in the feet and calves are in agreement with each other, and in disagreement with CEUS.

A) Perfusion recovery ratio of the ischemic:control limb measured by LDPI in the feet and calves before surgery and days 1, 4, 7, and 14 post-surgery. The calf has a slightly higher perfusion ratio before surgery, 1.09±0.03 vs 1.01±0.03 in the feet. Day one post-surgery, perfusion in the ischemic calf was greater than in the foot, 0.85±0.05 vs 0.72±0.03. Corresponding to this lesser initial reduction in perfusion, perfusion recovery was faster in the calves than the feet. (n=10) B) Perfusion recovery in the calf measured by LDPI and CEUS before surgery and days 1, 4, 7, and 14 post-surgery. By LDPI, perfusion returns to

normal within 4 days post-surgery. By CEUS, perfusion is more severely reduced at day 1, then improves modestly before achieving a plateau at ~50% of the control limb. (n=10)

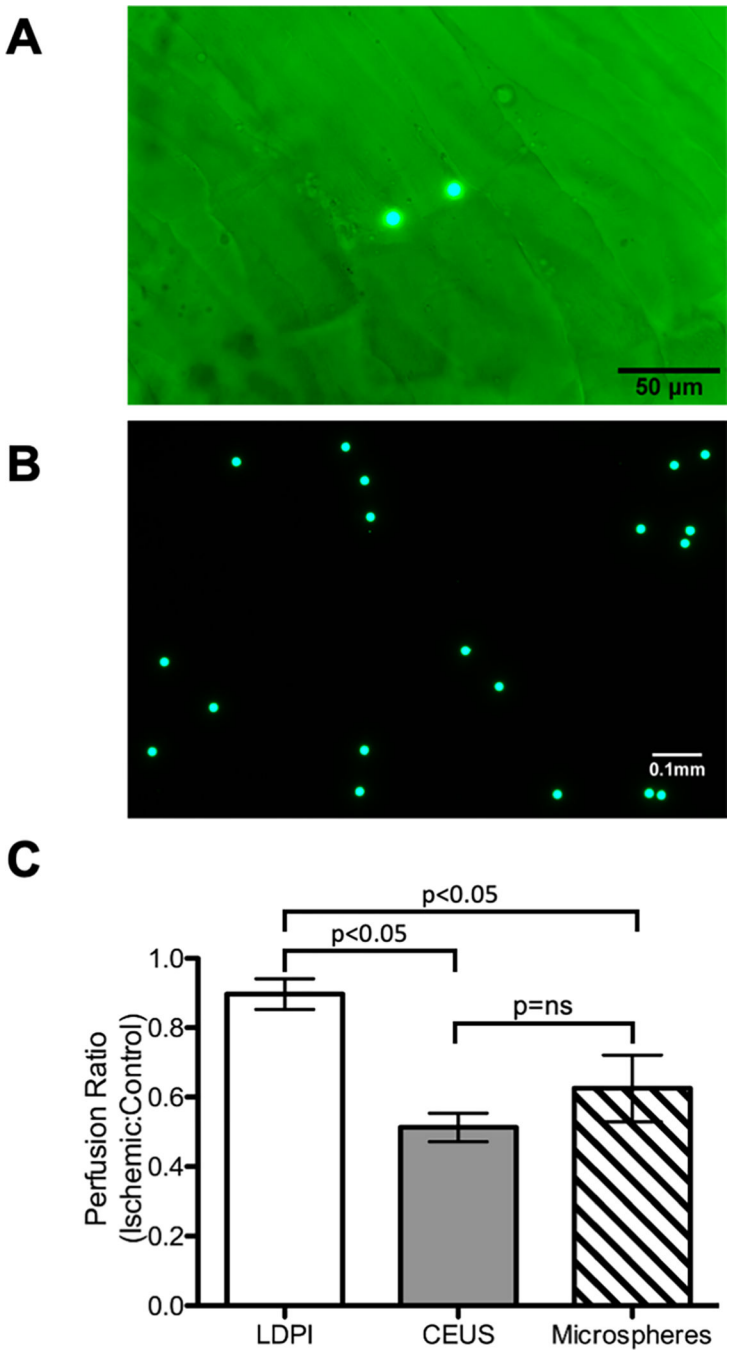

Fig 5. Fluorescent microspheres show reduced flow 14 days post-surgery in agreement with CEUS.

A) Green fluorescent microspheres in mouse skeletal muscle, imaged at 200x B) Green fluorescent microspheres, imaged at 100x. C) Comparison of perfusion ratios measured by LDPI, CEUS, and fluorescent microspheres at day 14 post-surgery. CEUS and fluorescent microspheres show good agreement with 50–60% perfusion recovery, whereas LDPI indicates nearly complete recovery (n=5, $p<0.05$). Statistical analysis was performed with a one-way ANOVA and Tukey's test for post-hoc analysis.

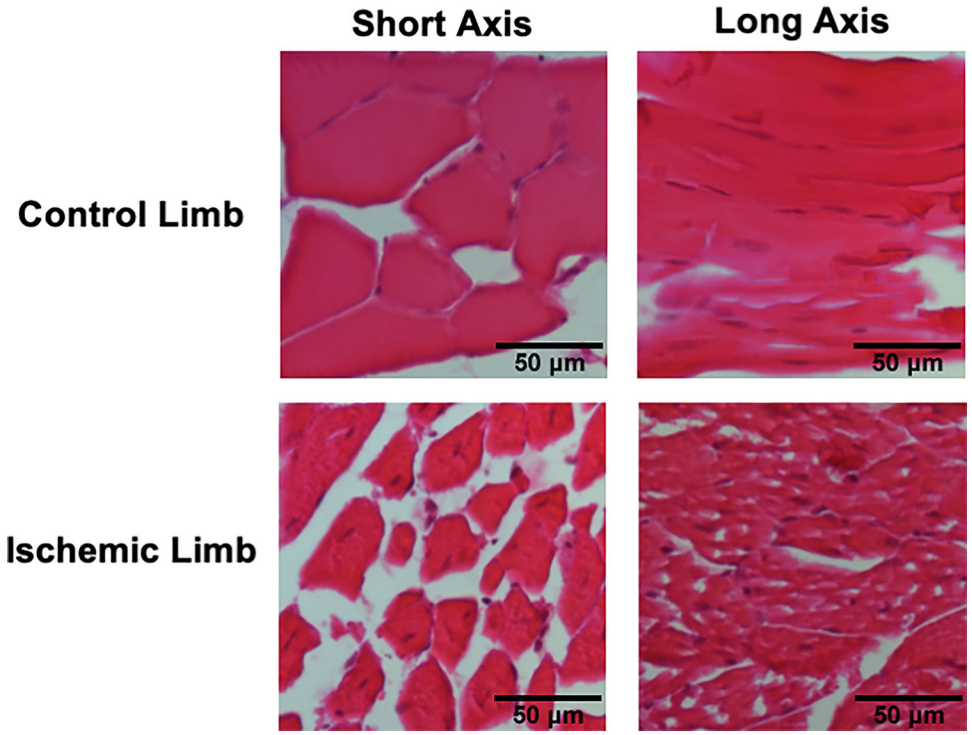

Fig 6. Muscle fibers remain abnormal 150 days post-surgery.

H&E staining of muscle 150 days post-surgery at 200x. Control limb muscle shows peripheral nuclei and uniform myofiber architecture (representative of n=5). Ischemic limb muscle shows irregular myofibers and many myofibers with centralized nuclei (representative of n=5).

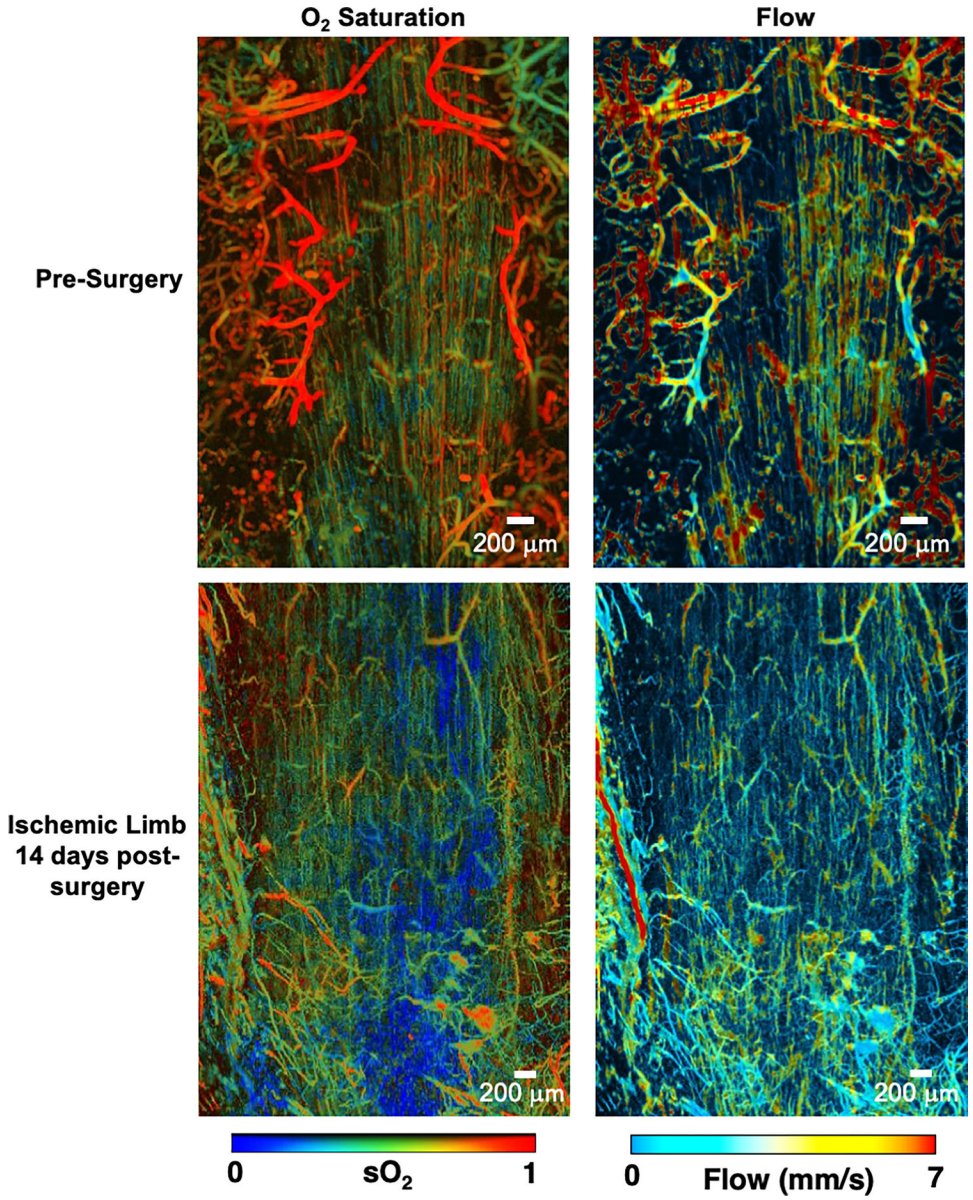

Fig 7. Photoacoustic microscopy shows disturbed morphology, flow, and oxygen saturation post-surgery.

Photoacoustic microscopy of the gastrocnemius muscle before and 14 days after HLI. Oxygen saturation and blood flow remain reduced 14 days post-surgery and the microvasculature becomes irregular and tortuous. Representative of n=3.